High-spin metal−cyanide clusters: species incorporating [Mn(salen)]$^+$ complexes as a source of anisotropy

Hye Jin Choi, Jennifer J. Sokol, Jeffrey R. Long*

Department of Chemistry, University of California, 209 Lewis Hall, Berkeley, CA 94720, USA

Received 10 June 2003; revised 7 September 2003

Abstract

The use of N,N'-ethylenebis(salycylideneiminato) (salen) complexes of Mn^{III} in assembling high-spin metal−cyanide coordination clusters with significant magnetic anisotropy is demonstrated. The reaction of [Mn(salen)(H$_2$O)$_2$]$^+$ with [Cr(CN)$_6$]$^{3-}$ in aqueous solution generates {Cr[CNMn(salen)(H$_2$O)]$_6$}[Cr(CN)$_6$]·6H$_2$O (**1**), a previously reported compound featuring a heptanuclear cluster with a distorted octahedral geometry. A fit to the variable-temperature magnetic susceptibility data for **1** revealed the presence of weak antiferromagnetic coupling of $J = -2.5$ cm^{-1} within the cluster, giving rise to an $S = 21/2$ ground state. In addition, variable-field magnetization data collected at low temperatures revealed the presence of magnetic anisotropy in the ground state, with the best fit yielding zero-field splitting parameters of $D = +0.19$ cm^{-1} and $|E| = 0.036$ cm^{-1}. A reaction intended to produce a direct analogue of **1** by employing [Fe(CN)$_6$]$^{3-}$ in place of [Cr(CN)$_6$]$^{3-}$ instead gave an unusually complex compound of formula {Fe(CN)$_4$[CNMn(salen)(MeOH)]$_2$}{[Mn(salen)(H$_2$O)]$_2$}[Mn(salen)(H$_2$O)(MeOH)]$_2$[Fe(CN)$_6$]·4H$_2$O (**2**). The crystal structure and magnetic properties of this compound are reported.
© 2003 Elsevier Ltd. All rights reserved.

1. Introduction

More than a decade ago, it was discovered that [Mn$_{12}$O$_{12}$(MeCO$_2$)$_{16}$(H$_2$O)$_4$]·2MeCO$_2$H·4H$_2$O, a molecular compound first reported by Lis [1], exhibits slow magnetic relaxation [2–4]. This behavior is now understood as arising from the effect of a negative axial zero-field splitting parameter, D, on a ground state of high spin, S. The resulting loss in degeneracy of the M_S levels leads to an energy barrier U for flipping the spin in an individual molecule from $M_S = +S$ to $M_S = -S$. In the Mn$_{12}$ cluster, an axial zero-field splitting parameter of approximately $D = -0.5$ cm^{-1} splits the M_S levels of its $S = 10$ ground state to give a barrier of $U = S^2|D| = 50$ cm^{-1} between $M_S = +10$ and $M_S = -10$. Molecules of this type display magnetic hysteresis at low temperatures [4], and consequently have been dubbed 'single-molecule magnets'; they are of interest for studying quantum tunneling of the magnetization [5–7], as well as for possible future applications in information storage and quantum computing [8]. In the past decade, many new examples of

metal-oxo clusters that behave as single-molecule magnets have been characterized [9–18]; however, none of these exhibit a larger spin-reversal barrier U.

In an effort to raise the barrier U in single-molecule magnets, some researchers have turned to the study of high-spin metal−cyanide coordination clusters [19–33]. The advantage here lies in the greater ability to control the formation of new cluster structures, owing to the preference of cyanide for adopting a linear bridging geometry between just two metal centers. Moreover, given this structural motif, the nature of the magnetic exchange coupling between neighboring metal centers is readily predicted [34,35]. Thus, as initially demonstrated with the cubic Prussian blue type solids [36–41], the magnetic properties of the product can be adjusted through a judicious choice of transition metal ions. This approach facilitates the synthesis of molecules with high-spin ground states, and indeed, the highest-spin clusters known to date are [(ROH)$_{24}$Mn$_9$M$_6$(CN)$_{48}$] (R = Me, M = Mo; R = Et, M = W), with $S = 51/2$ and $S = 39/2$, respectively [24,25].

While the ground state spin is an important contributor to the magnitude of the spin-reversal barrier in a single-molecule magnet, the barrier will not exist at all unless

the ground state also has a large negative D value. In metal–cyanide clusters, however, this axial zero-field splitting parameter can also be manipulated by selecting appropriate transition metal ions. For example, the trigonal prismatic cluster $[(Me_3tacn)_6MnCr_6(CN)_{18}]^{2+}$ ($Me_3tacn = N,N',N''$-trimethyl-1,4,7-triazacyclononane) has a ground state spin of $S = 13/2$ with $D \approx 0$ [27], but, upon substituting Mo^{III} for Cr^{III}, the analogous $[(Me_3tacn)_6MnMo_6(CN)_{18}]^{2+}$ cluster exhibits $S = 13/2$ with $D = -0.33$ cm^{-1} [30]. Accordingly, the latter molecule represents the first cyano-bridged single-molecule magnet, with an effective spin-reversal barrier of $U_{eff} = 10$ cm^{-1}, as determined from the frequency dependence of the AC magnetic susceptibility [30]. Thus, one approach to increasing the magnetic anisotropy for a non-cubic cluster geometry is simply to move down the periodic table, where the increased spin-orbit coupling will lead to an increase in the magnitude of D. (Note that accurately predicting the sign and magnitude of D in such complex molecules is really not yet possible.) An alternative approach is to use first row transition metal ions that have already been shown to create the necessary magnetic anisotropy in metal-oxo single-molecule magnets: metal ions such as Mn^{III}, V^{III}, and Co^{II}. Because, it provides the main contribution to the molecular anisotropy in $[Mn_{12}O_{12}(MeCO_2)_{16}(H_2O)_4]$, Mn^{III} is of particular interest for this purpose. While numerous cyano-bridged solids featuring Schiff base complexes of Mn^{III} have been reported [42–48], little attention has yet been paid to their potential in creating new single-molecule magnets.

Herein, we report some initial attempts to incorporate $[Mn(salen)]^+$ ($salen = N,N'$-ethylenebis(salycylideneiminato)) complexes into high-nuclearity metal–cyanide clusters, together with the magnetic properties of the resulting $Cr^{III}Mn_6^{III}$ and $Fe^{III}Mn_2^{III}$ cluster-containing products.

2. Experimental section

2.1. Preparation of compounds

All manipulations were carried out in air. The Schiff-base ligand N,N'-(bis(disalicylal)ethylenediamine) (salenH$_2$) was synthesized using a previously reported procedure [49]. The compound $[Mn(salen)(H_2O)]ClO_4 \cdot H_2O$ was then prepared by mixing $Mn(MeCO_2)_3 \cdot 2H_2O$, salenH$_2$ and LiClO$_4$ in a 1:1:1.5 molar ratio in MeOH, again according to a method described previously [50]. Water was distilled and deionized with a Milli-Q filtering system. All other reagents were obtained from commercial vendors and used without further purification. Infrared spectra were recorded using a Nicolet Avatar 360 FTIR spectrometer equipped with an attenuated total reflectance accessory.

2.1.1. {Cr[CNMn(salen)(H$_2$O)]$_6$}[Cr(CN)$_6$]·6H$_2$O (1)

This compound was synthesized in 73% yield by reacting $[Mn(salen)(H_2O)]ClO_4 \cdot H_2O$ with K$_3$[Cr(CN)$_6$] in aqueous solution, as previously described [47]. IR (solid, ATR): ν_{CN} (cyanide) 2129, 2123, ν_{CN}(imine) 1625, 1600 cm^{-1}. Anal. Calcd for $C_{108}H_{108}N_{24}O_{24}Cr_2Mn_6$: C, 50.68; H, 4.25; N, 13.13. Found: C, 50.48; H, 4.32; N, 12.94. The unit cell obtained for a dark brown block-shaped crystal of this compound was found to match that previously reported [47].

2.1.2. {Fe(CN)$_4$[CNMn(salen)(MeOH)]$_2$}{[Mn(salen) (H$_2$O)]$_2$}[Mn(salen)(H$_2$O)(MeOH)]$_2$[Fe(CN)$_6$]·4H$_2$O (2)

A procedure directly analogous to that employed in the preparation of **1** was used to synthesize this compound. A solution of $[Mn(salen)(H_2O)]ClO_4 \cdot H_2O$ (0.52 g, 1.1 mmol) in 45 ml of MeOH was added to a solution of K$_3$[Fe(CN)$_6$] (0.12 g, 0.37 mmol) in 4 ml of water. The mixture was filtered, and the dark brown filtrate was allowed to stand for 1 week. The resulting dark brown plate-shaped crystals were collected by filtration, washed with a 1:2 mixture of methanol and water, and dried in air to afford 0.28 g (59%) of product. IR (solid, ATR): ν_{CN} (cyanide) 2119, 2113, ν_{CN} (imine) 1621, 1599 cm^{-1}. Anal. Calcd for $C_{112}H_{116}Fe_2Mn_6N_{24}O_{24}$: C, 51.27; H, 4.46; N, 12.81. Found: C, 51.47; H, 4.49; N, 12.86. A single crystal of **2**·4MeOH suitable for X-ray analysis was obtained directly from the reaction mixture.

2.2. X-ray structure determination

A single crystal of **2**·4MeOH was coated with Paratone-N oil, attached to a glass fiber, transferred to a Siemens SMART diffractometer, and cooled to 119 K in a dinitrogen stream. Initial lattice parameters were obtained from a least-squares analysis of more than 30 centered reflections; these parameters were later refined against all data. The crystal did not show any significant decay during data collection. Data were integrated and corrected for Lorentz and polarization effects using SAINT and were corrected for absorption effects using SADABS.

The space group assignment was based on systematic absences, E statistics, and successful refinement of the structure. The structure was solved by direct methods with the aid of successive difference Fourier maps, and was refined against all data using the SHELXTL5.0 software package. The distance between the oxygen atoms (O6 and O14) of two water molecules in the structure was restrained to prevent them from moving within an unreasonably close distance of one another. Thermal parameters for all non-hydrogen atoms were refined anisotropically. Hydrogen atoms associated with solvate water were not included in the structural refinement. All other hydrogen atoms were assigned to ideal positions and refined by use of a riding model with an isotropic thermal parameter 1.2 times that of the attached carbon or nitrogen atom (1.5 times for methyl hydrogens).

The crystal and structure refinement parameters for **2**·4MeOH are: $C_{116}H_{132}Fe_2Mn_6N_{24}O_{28}$, $P\bar{1}$, $Z = 1$, $a = 14.985(8)$, $b = 14.880(8)$, and $c = 15.911(8)$ Å, $\alpha = 79.734(8)$, $\beta = 62.319(8)$, and $\gamma = 85.683(9)°$,

$V = 3091(3)$ Å^3, $d_{calc} = 1.487$ g/cm^3, no. reflections $= 6397$, no. parameters $= 800$, $R_1 = 0.0850$, $wR_2 = 0.1997$. This structure has been deposited with the Cambridge Crystallographic Data Centre as supplementary publication CCDC 219001. Copies of the data can be obtained free of charge on application to CCDC, 12 Union Road, Cambridge CB2 1EC, UK (Fax: +44-1223-336-033; e-mail: deposit@ccdc.cam.ac.uk).

2.3. Magnetic susceptibility measurements

DC magnetic susceptibility data were collected using a Quantum Design MPMS2 SQUID magnetometer at temperatures ranging from 5 to 295 K under an applied magnetic field of 1000 G. Data were corrected for diamagnetic contributions using Pascal's constants. For magnetization measurements, the sample was suspended in a petroleum jelly mull to prevent torquing of crystallites at high magnetic fields. A temperature-independent paramagnetism value of 0.0014 cgsu was assumed for **1** and the data were fit to a theoretical model using a relative error minimization routine (MAGFIT3.1) [51]. The program ANISOFIT2.0, which is freely available over the internet at http://alchemy.cchem.berkeley.edu, was used in fitting the magnetization data for compound **1** [28]. All coupling constants reported herein are based on exchange Hamiltonians of the form $\hat{H} = -2J\hat{S}_i \cdot \hat{S}_j$.

3. Results and discussion

3.1. Syntheses and structures

The compounds {Cr[CNMn(salen)(H$_2$O)]$_6$}[Cr(CN)$_6$]·6H$_2$O (**1**) and {Fe(CN)$_4$[CNMn(salen)(MeOH)]$_2$}{[Mn(salen)(H$_2$O)]$_2$}[Mn(salen)(H$_2$O)(MeOH)]$_2$[Fe(CN)$_6$]·4H$_2$O (**2**) were synthesized by the dropwise addition of an aqueous solution of K$_3$[M(CN)$_6$] (M = Cr or Fe) into a methanol solution of [Mn(salen)(H$_2$O)]ClO$_4$·H$_2$O. As the amount of water increased in the reaction solution, the crystals began to form more and more rapidly. Upon standing for one week, the products were isolated as dark brown crystals. The infrared spectrum of **2** displays ν_{CN} stretching bands at 2119 and 2113 cm^{-1}, indicating that the +3 oxidation state of iron is maintained in the product.

The unit cell parameters for a single crystal of **1** revealed it to be identical to a previously reported structure [47]. Thus, the compound contains the heptanuclear cluster {Cr[CNMn(salen)(H$_2$O)]$_6$}$^{3+}$, in which a central [Cr(CN)$_6$]$^{3-}$ unit is coordinated through each of its nitrogen atoms to a salen-bound Mn^{III} center (see Fig. 1). As usual for such Schiff base complexes, each Mn^{III} center shows a strong Jahn–Teller type distortion, with the elongated bond lengths occurring along the axis perpendicular to the plane of the salen ligand. The molecule resides on a $\bar{3}$ symmetry
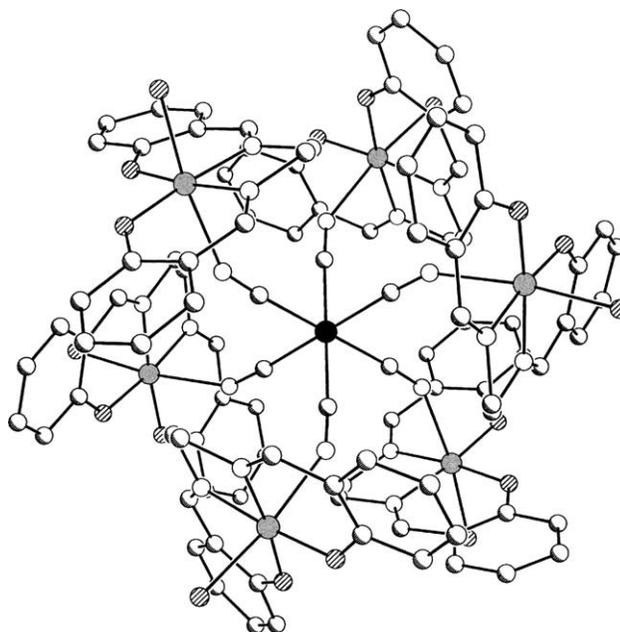

Fig. 1. Structure of the {Cr[CNMn(salen)(H$_2$O)]$_6$}$^{3+}$ cluster in **1** [47]. Black, gray, shaded, white, and hatched spheres represent Cr, Mn, C, N, and O atoms, respectively; H atoms are omitted for clarity.

site in the crystal, and exhibits bent Mn–N≡C angles of 149.9(4)° that lead to a significant departure from O_h symmetry for the [Cr(CNMn)$_6$]$^{15+}$ cluster core. An isolated [Cr(CN)$_6$]$^{3-}$ complex balances the charge of the cluster.

Despite its analogous preparation and composition, X-ray analysis of a single crystal of **2**·4MeOH revealed a structure quite different from that in **1**. This structure instead features a trinuclear {Fe(CN)$_4$[CNMn(salen)(MeOH)]$_2$}$^{1-}$ cluster, which has cocrystallized with a dimeric {[Mn(salen)(H$_2$O)]$_2$}$^{2+}$ complex, two isolated [Mn(salen)(MeOH)(H$_2$O)]$^+$ complexes, and one isolated [Fe(CN)$_6$]$^{3-}$
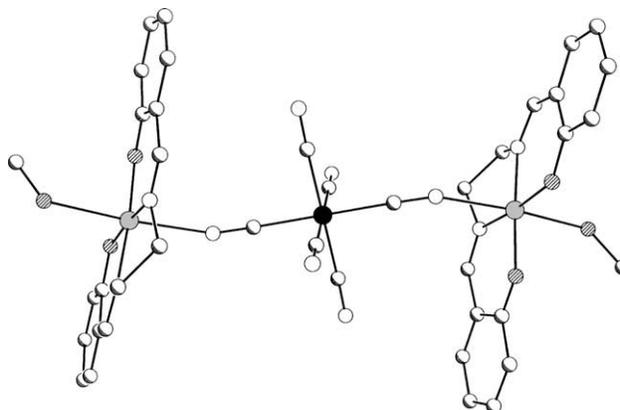
Fig. 2. Structure of the {Fe(CN)$_4$[CNMn(salen)(MeOH)]$_2$}$^{1-}$ cluster in **2**·4MeOH. Black, gray, shaded, white, and hatched spheres represent Fe, Mn, C, N, and O atoms, respectively; H atoms are omitted for clarity. The molecule resides on a crystallographic inversion center. Selected mean interatomic distances (Å) and angles (deg): Fe–C 1.940(7), C≡N 1.150(9), Mn–N$_{CN}$ 2.30(1), Mn–N$_{salen}$ 1.981(7), Mn–O$_{salen}$ 1.888(6), Mn–O$_{MeOH}$ 2.365(9), C–Fe–C 90.0(2), Fe–C–N 178.3(7), Mn–N≡C 149(1).
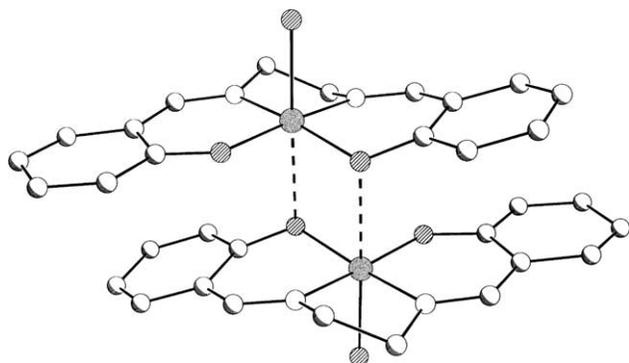
Fig. 3. Structure of the $\{[Mn(salen)(H_2O)]_2\}^{2+}$ complex in $2\cdot4MeOH$. Gray, shaded, white, and hatched spheres represent Mn, C, N and O atoms, respectively; H atoms are omitted for clarity. Selected mean interatomic distances (Å) and angles (deg): $Mn-N_{salen}$ 1.966(8), $Mn-O_{salen}$ 1.880(6), $Mn-O_{water}$ 2.17(1), $Mn\cdots O$ 2.67(1), $Mn\cdots Mn$ 3.419(5) $Mn-O\cdots Mn$ 95.4(4).

Fig. 4. Magnetic behavior of $\{Cr[CNMn(salen)(H_2O)]_6\}[Cr(CN)_6]\cdot6H_2O$ (**1**), as measured in an applied field of 1000 G. Squares and circles represent data before and after subtracting the paramagnetic contribution of the spin-isolated $[Cr(CN)_6]^{3-}$ counteranion. The solid line represents a calculated fit to the adjusted data.

complex. A closely related structure, differing only in the number of solvate molecules, has been reported previously [42]. Fig. 2 displays the structure of the FeMn$_2$ cluster in $2\cdot4MeOH$. Here, a central $[Fe(CN)_6]^{3-}$ moiety is coordinated through two *trans* nitrogen atoms to salen-bound Mn^{III} centers, giving rise to a linear geometry of a type frequently encountered before [42,45,46]. Once again, each Mn^{III} center displays shorter bonds to the salen donor atoms than to the axially coordinated cyanide and methanol ligands (see legend of Fig. 2). Although, only two salen complexes surround the central hexacyanometalate unit, the Mn–N≡C angle of 149(1)° is still very bent. The structure of the Mn$_2$ complex in **2** is depicted in Fig. 3, and consists of two $[Mn(salen)(H_2O)]^+$ units that are dimerized through mutual axial interactions between a Mn^{III} center and a phenoxy oxygen atom of the neighboring salen ligand. Therein, the $Mn\cdots O$ separation of 2.671(9) Å and Mn–O$\cdots$Mn angle of 95.4(4)°, respectively, differ notably from the corresponding parameters of 2.412(6) Å and 100.6(2)° in $[Mn(salen)(H_2O)]_2(ClO_4)_2$ [52].

3.2. Magnetic properties of *1*

The magnetic properties of $\{Cr[CNMn(salen)(H_2O)]_6\}$ $[Cr(CN)_6]\cdot6H_2O$ (**1**) have been presented and analyzed in a previous report by Xu and co-workers [47]. Therein, the compound was claimed to exhibit an unusually high effective magnetic moment of $\mu_{eff} = 22.78$ μ_B ($\chi_MT = 64.88$ cm^{3}K/mol) at room temperature. With decreasing temperature, this moment was observed to drop steadily, reaching a local minimum at 47 K, before rising briefly to a local maximum of ca. 14 μ_B (= 25 cm^{3}K/mol) at 13 K and then plummeting toward zero. This behavior was interpreted as indicating the CrMn$_6$ cluster to possess 'a strong antiferromagnetic interaction with a $S = 21/2$ ground state at room temperature'. In view of these unusual results and conclusions, we have remeasured and reanalyzed the magnetic properties of the compound.
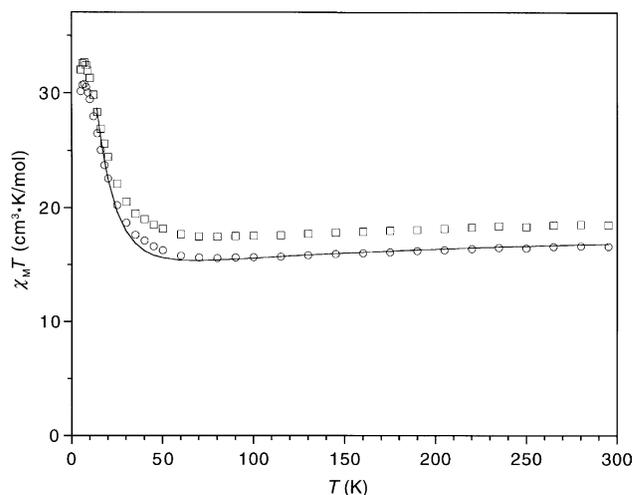
As measured in an applied field of 1000 G, the magnetic susceptibility data we obtained for compound **1** differ dramatically from the previously reported data. Fig. 4 shows plots of χ_MT both before (squares) and after (circles) subtracting a contribution of 1.876 cm^3 K/mol assumed for the $[Cr(CN)_6]^{3-}$ counteranion. The CrMn$_6$ cluster exhibits a χ_MT value of 16.6 cm^3 K/mol at 295 K, which is slightly below the value of 19.9 cm^3 K/mol expected for one Cr^{III} ($S = 3/2$) and six high-spin Mn^{III} ($S = 2$) centers in the absence of any exchange coupling. As the temperature is lowered, χ_MT gradually decreases, reaching a shallow minimum at ca. 70 K before rising steeply. This behavior is consistent with the expected [34,35] antiferromagnetic coupling between Cr^{III} and the six surrounding Mn^{III} centers to give an $S = 21/2$ ground state. Note, however, that the maximum value of $\chi_MT = 30.8$ cm^{3}K/mol attained at 7 K is significantly lower than the spin-only value of 60.4 cm^3 K/mol expected for an $S = 21/2$ ground state. This reduced moment, together with the downturn in χ_MT below 7 K, is attributed primarily to the presence of zero-field splitting in the ground state. The susceptibility data above 14 K were fit using MAGFIT3.1 and an exchange Hamiltonian of the following form.

$$\hat{H}=-2J[\hat{S}_{Cr}\cdot(\hat{S}_{Mn(1)}+\hat{S}_{Mn(2)}+\hat{S}_{Mn(3)}+\hat{S}_{Mn(4)}+\hat{S}_{Mn(5)}+\hat{S}_{Mn(6)}]$$
(1)

The best fit, corresponding to the solid line in Fig. 4, gave parameters of $J= -2.5$ cm^{-1} and $g=1.86$. This coupling constant is comparable to but slightly greater in magnitude than the value of $J= -1.1$ cm^{-1} observed for the tetra-nuclear cluster $[Cr(CN)_3(CNMnL)_3]$, where L is a dianionic pentadentate ligand related to salen [53]. Unfortunately, the structure of this molecule, which presumably features analogous Cr^{III}–CN–Mn^{III} linkages, is not available for

comparison. Thus, while the CrMn$_6$ cluster in **1** does possess an unusually high-spin ground state of $S = 21/2$, the antiferromagnetic coupling within the molecule is in fact very weak, such that spin-excited states are thermally populated even at temperatures well below room temperature.

The nature of the zero-field splitting in the ground state of the CrMn$_6$ cluster in compound **1** was further examined through variable-field magnetization measurements performed at low temperatures. The corrected magnetization data are plotted in Fig. 5, where the clear deviations from a single Brillouin function signify the presence of a substantial zero-field splitting. It is important to note that this anisotropy arises despite the high symmetry of the cluster, which deviates from an octahedral core geometry only by virtue of its bent cyanide bridges. Assuming an $S = 21/2$ ground state and negligible population of excited spin states, the data with $T \leq 4$ K were fit at all fields simultaneously using ANISOFIT2.0 [28]. The best fit, shown as the solid lines in Fig. 5, matched the data closely, giving $D = +0.19$ cm^{-1}, $|E| = 0.036$ cm^{-1}, and $g = 1.588$ [54]. Although, the sign of D is generally not reliably determined from such magnetization data, in this case no reasonable fit could be obtained when constraining D to be negative. Thus, while the D values for mononuclear Schiff-base complexes of Mn^{III} have typically been found to fall in the range of -1.0 to -3.0 cm^{-1} [55,56], the compilation of single-ion anisotropy parameters appears to give rise to a positive D value for the ground state of the Cr^{III}Mn$_6^{III}$ cluster. As a consequence, the cluster is not expected to behave as a single-molecule magnet. Indeed, AC magnetic suscepti-bility measurements performed at temperatures as low as 1.9 K and frequencies in the range 1000–1500 Hz confirmed the absence of an out-of-phase signal.
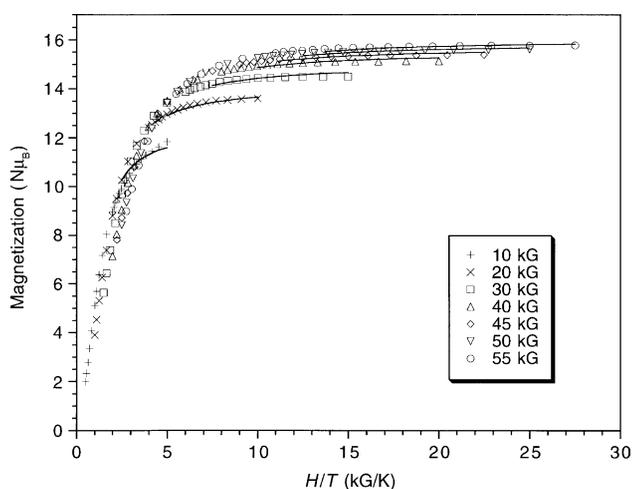

Fig. 5. Magnetization data for a constrained powder sample of {Cr[CNMn(salen)(H$_2$O)]$_6$}[Cr(CN)$_6$]·6H$_2$O (**1**), after subtracting the Brillouin contribution from the [Cr(CN)$_6$]$^{3-}$ counteranion. Solid lines correspond to calculated fits to the data.
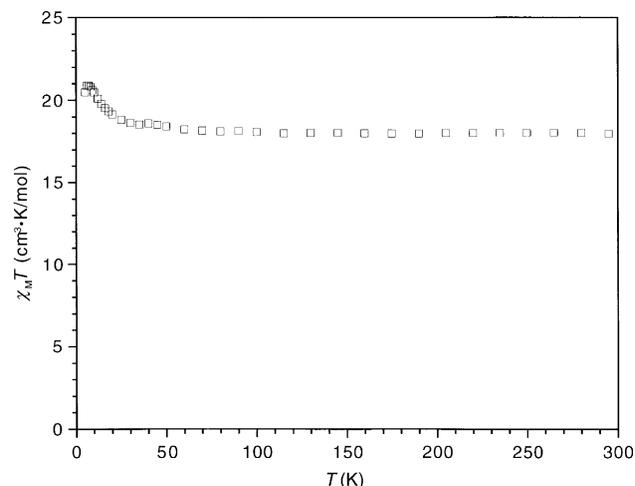

Fig. 6. Magnetic behavior of compound **2**, as measured in an applied field of 1000 G.

3.3. Magnetic properties of 2

The magnetic behavior of **2** is difficult to interpret, owing to the presence of two distinct clusters, {Fe(CN)$_4$[CNMn(salen)(MeOH)]$_2$}$^{1-}$ and {[Mn(salen)(H$_2$O)]$_2$}$^{2+}$, both of which are likely to exhibit exchange coupling. The variation of $\chi_M T$ with temperature for this compound is plotted in Fig. 6. At 295 K, $\chi_M T = 18.0$ cm^{3}K/mol, which is only slightly below the spin-only value of 18.8 cm^3 K/mol expected for two low-spin Fe^{III} ($S = 1/2$) and six high-spin Mn^{III} ($S = 2$) centers in the absence of any exchange coupling. The difference is most likely just a consequence of g being less than 2.00. As the temperature is lowered, $\chi_M T$ increases gradually, reaching a maximum of 20.9 cm^3 K/mol at 7 K, before decreasing to 20.5 cm^3 K/mol at 5 K. This behavior suggests the presence of weak ferromagnetic exchange interactions within the compound, possibly with the effects of zero-field splitting associated with the Mn^{III} centers taking over below 7 K. The result is very reasonable, in view of the magnetic properties previously observed for related clusters. With a linear geometry similar to that encountered in **2**, clusters of the type {Fe(CN)$_4$[CNMn(5-X-salen)(H$_2$O)]$_2$}$^{1-}$ (X = Cl, Br) exhibit weak ferromagnetic coupling with $J \approx 4$ cm^{-1} [42,44,45]. In addition, the dimeric units in [Mn(salen)(H$_2$O)]$_2$(ClO$_4$)$_2$ also display weak ferromagnetic coupling, with $J = 6.3$ cm^{-1} [52]. With both types of clusters present in **2**, however, J values are not readily extracted from the magnetic data for comparison.

4. Outlook

The foregoing results demonstrate the utility of Schiff base complexes of Mn^{III} in the synthesis of metal–cyanide coordination clusters possessing a high-spin ground state with significant magnetic anisotropy. Owing to the weak axial bonds associated with these complexes, it can be

anticipated that subtle changes in the reactants and reaction conditions will lead to cyano-bridged clusters with very different geometries. These differences will certainly affect the nature of the anisotropy in the ground state, potentially resulting in clusters with a large negative zero-field splitting that behave as single-molecule magnets. Ultimately, it may also be possible to increase both the magnitude of the zero-field splitting and the strength of the magnetic exchange coupling in such species through the use of second- or third-row transition metal ions [28,30].

References

[1] T. Lis, Acta Crystallogr. B 36 (1980) 2042.
[2] A. Caneschi, D. Gatteschi, R. Sessoli, A.L. Barra, L.C. Brunel, M. Guillot, J. Am. Chem. Soc. 113 (1991) 5873.
[3] R. Sessoli, H.-L. Tsai, A.R. Schake, S. Wang, J.B. Vincent, K. Folting, D. Gatteschi, G. Christou, D.N. Hendrickson, J. Am. Chem. Soc. 115 (1993) 1804.
[4] R. Sessoli, D. Gatteschi, A. Caneschi, M.A. Novak, Nature 365 (1993) 141.
[5] J.R. Friedman, M.P. Sarachik, J. Tejada, R. Ziolo, Phys. Rev. Lett. 76 (1996) 3830.
[6] L. Thomas, F. Lionti, R. Ballou, D. Gatteschi, R. Sessoli, B. Barbara, Nature 383 (1996) 145.
[7] D. Gatteschi, R. Sessoli, Angew. Chem. Int. Ed. 42 (2003) 268.
[8] M.N. Leuenberger, D. Loss, Nature 410 (2001) 789.
[9] H.J. Eppley, H.-L. Tsai, N. de Vries, K. Folting, G. Christou, D.N. Hendrickson, J. Am. Chem. Soc. 117 (1995) 301.
[10] S.M.J. Aubin, M.W. Wemple, D.M. Adams, H.-L. Tsai, G. Christou, D.N. Hendrickson, J. Am. Chem. Soc. 118 (1996) 7746.
[11] A.-L. Barra, P. Debrunner, C.E. Schultz, R. Sessoli, Europhys. Lett. 35 (1996) 133.
[12] S.L. Castro, Z. Sun, C.M. Grant, J.C. Bolinger, D.N. Hendrickson, G. Christou, J. Am. Chem. Soc. 120 (1998) 2365.
[13] A.-L. Barra, A. Caneschi, A. Cornia, F. Fabrizi de Biani, D. Gatteschi, C. Sangregorio, R. Sessoli, L. Sorace, J. Am. Chem. Soc. 121 (1999) 5302.
[14] J.C. Goodwin, R. Sessoli, D. Gatteschi, W. Wernsdorfer, A.K. Powell, S.L. Heath, J. Chem. Soc. Dalton Trans. (2000) 1835.
[15] C. Cadiou, M. Murrie, C. Paulsen, V. Villar, W. Wernsdorfer, R.E.P. Winpenny, Chem. Commun. (2001) 2666.
[16] C. Boskovic, E.K. Brechin, W.E. Streib, K. Folting, J.C. Bollinger, D.N. Hendrickson, G. Christou, J. Am. Chem. Soc. 124 (2002) 3725.
[17] E.K. Brechin, M. Soler, J. Davidson, D.N. Hendrickson, S. Parsons, G. Christou, Chem. Commun. (2002) 2252.
[18] S.T. Ochsenbein, M. Murrie, E. Rusanov, H. Stoeckli-Evans, C. Sekine, H.U. Güdel, Inorg. Chem. 41 (2002) 5133.
[19] T. Mallah, C. Auberger, M. Verdaguer, P. Veillet, J. Chem. Soc., Chem. Commun. (1995) 61.
[20] A. Scuiller, T. Mallah, M. Verdaguer, A. Nivorzkhin, J.-L. Tholence, P. Veillet, New J. Chem. 20 (1996) 1.
[21] J.L. Heinrich, P.A. Berseth, J.R. Long, Chem. Commun. (1998) 1231.
[22] H. Oshio, O. Tamada, H. Onodera, T. Ito, T. Ikoma, S. Tero-Kubota, Inorg. Chem. 38 (1999) 5686.
[23] P.A. Berseth, J.J. Sokol, M.P. Shores, J.L. Heinrich, J.R. Long, J. Am. Chem. Soc. 122 (2000) 9655.
[24] Z.J. Zhong, H. Seino, Y. Mizobe, M. Hidai, A. Fujishima, S. Ohkoshi, K. Hashimoto, J. Am. Chem. Soc. 122 (2000) 2952.
[25] J. Larionova, M. Gross, M. Pilkington, H. Andres, H. Stoeckli-Evans, H.U. Güdel, S. Decurtins, Angew. Chem. Int. Ed. 39 (2000) 1605.
[26] R.J. Parker, L. Spiccia, K.J. Berry, G.D. Fallon, B. Moubaraki, K.S. Murray, Chem. Commun. (2001) 333.
[27] J.L. Heinrich, J.J. Sokol, A.G. Hee, J.R. Long, J. Solid State Chem. 159 (2001) 293.
[28] M.P. Shores, J.J. Sokol, J.R. Long, J. Am. Chem. Soc. 124 (2002) 2279.
[29] R. Lescouëzec, J. Vaisserman, F. Lloret, M. Julve, M. Verdaguer, Inorg. Chem. 41 (2002) 5943.
[30] J.J. Sokol, A.G. Hee, J.R. Long, J. Am. Chem. Soc. 124 (2002) 7656.
[31] J.Y. Yang, M.P. Shores, J.J. Sokol, J.R. Long, Inorg. Chem. 42 (2003) 1403.
[32] V. Marvaud, C. Decroix, A. Scuiller, C. Guyard-Duhayon, J. Vaissermann, F. Gonnet, M. Verdaguer, Chem. Eur. J. 9 (2003) 1678.
[33] C.P. Berlinguette, D. Vaughn, C. Cañada-Vilalta, J.R. Galán-Mascarós, K.R. Dunbar, Angew. Chem. Int. Ed. 42 (2003) 1523.
[34] W.R. Entley, C.R. Treadway, G.S. Girolami, Mol. Cryst. Liq. Cryst. 273 (1995) 153.
[35] H. Weihe, H.U. Güdel, Comments Inorg. Chem. 22 (2000) 75.
[36] V. Gadet, T. Mallah, I. Castro, M. Verdaguer, J. Am. Chem. Soc. 114 (1992) 9213.
[37] T. Mallah, S. Thiébaut, M. Verdaguer, P. Veillet, Science 262 (1993) 1554.
[38] W.R. Entley, G.S. Girolami, Science 268 (1995) 397.
[39] S. Ferlay, T. Mallah, R. Ouahès, P. Veillet, M. Verdaguer, Nature 378 (1995) 701.
[40] Ø. Hatlevik, W.E. Buschmann, J. Zhang, J.L. Manson, J.S. Miller, Adv. Mater. 11 (1999) 914.
[41] S.M. Holmes, G.S. Girolami, J. Am. Chem. Soc. 121 (1999) 5593.
[42] H. Miyasaka, N. Matsumoto, H. Okawa, N. Re, E. Gallo, C. Floriani, J. Am. Chem. Soc. 118 (1996) 981.
[43] N. Re, E. Gallo, C. Floriani, H. Miyasaka, N. Matsumoto, Inorg. Chem. 35 (1996) 6004.
[44] H. Miyasaka, N. Matsumoto, N. Re, E. Gallo, C. Floriani, Inorg. Chem. 36 (1997) 670.
[45] H. Miyasaka, H. Ieda, N. Matsumoto, N. Re, R. Crescenzi, C. Floriani, Inorg. Chem. 37 (1998) 255.
[46] M. Clemente-León, E. Coronado, J.R. Galán-Mascarós, C.J. Gómez-García, T. Woike, J.M. Clemente-Juan, Inorg. Chem. 40 (2001) 87.
[47] X. Shen, B. Li, J. Zou, Z. Xu, Trans. Met. Chem. 27 (2002) 372.
[48] H. Miyasaka, H. Ieda, N. Matsumoto, K.-I. Sugiura, M. Yamashita, Inorg. Chem. 42 (2003) 3509.
[49] H. Diehl, C.C. Hach, Inorg. Syn. 3 (1950) 196.
[50] N. Matsumoto, N. Takemoto, A. Ohyoshi, H. Okawa, Bull. Chem. Soc. Jpn 61 (1988) 2984.
[51] E. A. Schmitt, PhD Thesis, University of Illinois at Urbana-Champaign, 1995.
[52] H.-L. Shyu, H.-H. Wei, Y. Wang, Inorg. Chim. Acta 290 (1999) 8.
[53] A. Marvilliers, T. Mallah, E. Riviere, S. Parsons, C. Munoz, K.E. Vostrikova, Mol. Cryst. Liq. Cryst. 335 (1999) 483.
[54] It is not clear why the ground state should exhibit this somewhat lower value of g. When g was fixed at 1.86 (the value obtained from fitting the susceptibility data) the best fit to the data was noticeably worse and gave zero-field splitting parameters of $D = +1.95 \, \mathrm{cm}^{-1}$ and $|E| = 0.11 \, \mathrm{cm}^{-1}$.
[55] D.V. Behere, S. Mitra, Inorg. Chem. 19 (1980) 992.
[56] B.J. Mennedy, K.S. Murray, Inorg. Chem. 24 (1985) 1552.